

Control of the nonlinear carrier response time of AlGaAs photonic crystal waveguides by sample design

P. Murzyn,^{a)} A. Z. Garcia-Deniz, D. O. Kundys, A. M. Fox, J.-P. R. Wells, D. M. Whittaker, and M. S. Skolnick

Department of Physics and Astronomy, University of Sheffield, Hounsfield Road, Sheffield S3 7RH, United Kingdom

T. F. Krauss

School of Physics and Astronomy, University of St. Andrews, St. Andrews KY16 9SS, United Kingdom

J. S. Roberts

Department of Electronic and Electrical Engineering, University of Sheffield, Mappin Street, Sheffield S1 3JD, United Kingdom

(Received 29 November 2005; accepted 18 February 2006; published online 4 April 2006)

We have used reflection geometry pump-probe spectroscopy to investigate the free carrier response time of AlGaAs high refractive index contrast one-dimensional photonic crystal waveguides. We have observed pump-induced shifts of photonic resonances in the near infrared spectral region, and have studied the dependence of the decay time on the sample parameters. We find that the response time can be varied from 8 to 33 ps by changing the structure period and etch depth. This, combined with the large changes observed in the reflectivity, demonstrates excellent potential for application as ultrafast photonic switches with a controllable recovery time. © 2006 American Institute of Physics. [DOI: 10.1063/1.2191955]

Photonic crystals (PCs) have been a very active research area, ever since they were first proposed by Yablonovitch¹ and John² in 1987. The unique properties of PCs enable a whole range of possibilities for controlling the propagation and emission of light. These properties make PCs particularly well suited for use as ultrafast photonic switches in all-optical telecommunications networks.³ Theoretical proposals to implement such switches by using optically induced shifts of photonic resonances^{4–7} have now been demonstrated in small^{8,9} and high^{10–15} refractive index contrast PCs. Despite the work carried out to date, the nonlinear properties of the PCs are not fully understood, especially as regards the dependence of these properties on the detailed design of the structures.

In our previous work we have shown that it is possible to modulate the reflectivity of a photonic crystal waveguide (PCW) by generating free carriers in the core.^{13,14} The pump pulse with high intensity creates a large carrier population in the conduction band (i.e., by single or two photon absorption) and these carriers then modify the optical properties. The refractive index change alters the photonic band structure and results in a shift of the photonic resonance accompanied by large changes in the reflectivity. The decay time for a two-dimensional (2D) crystal was found to be around 10 ps. This fast decay was attributed to surface recombination at the air holes. In this Letter, we investigate the response time of the free carrier nonlinearities in a series of high refractive index contrast one-dimensional (1D) AlGaAs PCWs with a systematic variation of the period, air-fill factor, and etch depth. The aim was to improve the understanding of the surface recombination effects and to determine the degree of control that can be exercised over them. The results indicate that the response time depends strongly on all

of the parameters, allowing extra scope for device optimization by choice of the design parameters of the PCW.

The PCW investigated here is shown schematically in Fig. 1. The PCW was grown by metal organic vapor phase epitaxy (MOVPE). The core was 400 nm thick and consisted of an active region of five periods of 9.6 nm thick $\text{In}_{0.12}\text{Al}_{0.2}\text{Ga}_{0.68}\text{As}$ quantum wells with 10 nm thick $\text{Al}_{0.2}\text{Ga}_{0.8}\text{As}$ barriers surrounded on both sides by approximately 150 nm of $\text{Al}_{0.2}\text{Ga}_{0.8}\text{As}$. The purpose of the quantum wells in the core was to enhance the magnitude of the refractive index change induced by the carriers. The waveguide was realized with air acting as the top cladding and a 1500 nm thick $\text{Al}_{0.6}\text{Ga}_{0.4}\text{As}$ layer as the bottom cladding. The structure was capped with a 10 nm layer of GaAs to minimize oxidation. Room temperature photoluminescence measurements showed excitonic emission around 790–800 nm.

Photonic crystals were patterned onto the top surface of the wafer by electron-beam lithography and were then etched by chemically assisted ion-beam etching. A variety of 1D photonic structures with different periods and air fill factors were patterned onto the same wafer. Each photonic structure was a square with dimensions of $80 \times 80 \mu\text{m}^2$, surrounded

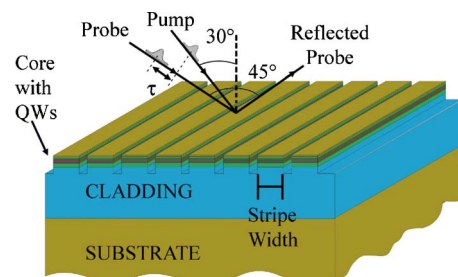


FIG. 1. (Color online) Experimental geometry of the pump-probe technique and the layer structure of the sample.

^{a)}Electronic mail: p.murzyn@sheffield.ac.uk

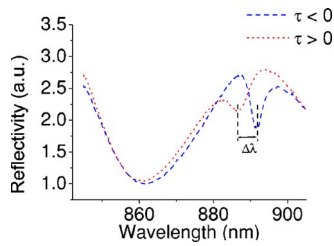


FIG. 2. (Color online) Representative reflectivity spectra at negative and positive time delays for a PCW with a stripe width of 704 nm and an etch depth of 850 nm. The Wavelength shift ($\Delta\lambda$) of the photonic resonance is shown.

by a deeply etched air moat of width $20\ \mu\text{m}$. The period a ranged from 330 to 880 nm, while the air-fill factor f was varied from 10%–30%. These two parameters together determine the stripe width w according to $w = a(1 - f)$. The etch depth was either 100 or 850 nm. In the former case, the etching stopped in the core region, while in the latter, the pattern penetrated down into the bottom cladding.

The photonic structures were investigated by external-coupling reflectivity measurements. This technique provides information about the photonic band structure by coupling to the leaky modes in the PCW structure. The incident light has to satisfy the phase-matching condition $k_{\parallel} = (\omega/c)\sin\theta$, where k_{\parallel} is the in-plane wave vector, ω is the angular frequency, and θ is the coupling angle as shown in Fig. 1. Parts of the band structure of the PCW can then be mapped out by varying θ .

Time-resolved measurements were carried out at room temperature by a pump-probe technique in reflection geometry.^{13,14} The pump beam was generated by a TOPAS optical parametric amplifier (OPA) with a tuning range from 240 nm to $18\ \mu\text{m}$. The TOPAS OPA was pumped by a regenerative-amplified, mode-locked, Ti:sapphire laser operating at 800 nm with a pulse width of 130 fs and a repetition rate of 1 kHz. The pump beam wavelength was set to 810 nm and was focused on to the sample with a spot size $< 200\ \mu\text{m}$ at an incident angle of 30° . The pump fluence was set to $0.45\ \text{mJ}/\text{cm}^2$.

A small part of the Ti:sapphire beam was used to generate a femtosecond white light continuum in a thin sapphire plate. The resulting beam was collimated with a divergence angle $< 2^\circ$ and was used as the probe in the time-resolved measurements. The probe beam was incident on the sample at an angle of 45° . The surface-reflected beam was then magnified and imaged onto a pinhole, thus allowing the signal from an individual photonic crystal to be collected. The spatially filtered signal was then fed into a spectrometer and detected by a charge-coupled device (CCD). A reference beam was extracted from the white light continuum and used to normalize the signal, thus removing wavelength-dependent systematic backgrounds and noise due to pulse energy fluctuations.

Typical pump-probe reflectivity spectra are shown in Fig. 2 for two values of the probe time delay τ . Negative values of τ indicate that the probe arrived before the pump pulse, and that the sample was therefore unexcited. In Fig. 2 a photonic feature at 892 nm for negative τ is observed to shift to shorter wavelengths for $\tau > 0$. This shift is caused by the refractive index change associated with the free carriers generated by the pump pulse.^{13,14} By plotting the wavelength shift $\Delta\lambda$ of the photonic resonance against τ , graphs such as

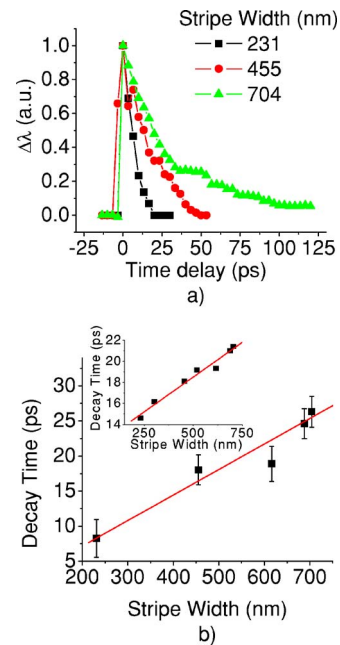


FIG. 3. (Color online) (a) Wavelength shift $\Delta\lambda$ of the photonic resonance vs probe time delay τ for three different stripe widths. The etch depth was 850 nm in all three cases. $\Delta\lambda$ has been normalized with $\Delta\lambda(\tau)$ set to unity at zero time delay. (b) Decay time vs stripe width for a constant etch depth of 850 nm. The inset shows the results of a simple in-plane diffusion model. The red lines, in both the main graph and inset, represent a linear fit to the experimental and modeled points, respectively.

those shown in Figs. 3(a) and 4 may be obtained. The response time for each for the samples can then be determined by fitting the decay of $\Delta\lambda$.

Figure 3(a) shows decay curves for three representative values of the stripe width w at a constant etch depth of 850 nm, while Fig. 3(b) plots the decay times extracted from the data against w . A clear linear dependence exists between the decay times and the stripe width. The times obtained are too short for bulk recombination. Additionally, the samples were processed in a similar manner and conditions, ruling out that the recombination changes were caused by the processing. (N.B. No change in the response time was observed for different e-beam exposure times). The results in Fig. 3 therefore can be understood by invoking the surface recombination model proposed to explain the rapid decay time observed in our previous experiments on 2D structures.^{13,14} In similar excitation conditions, we expect the free carriers to have the same diffusion speed and the same lifetime. The decay time in the PCW is then expected to scale with the average distance that the carriers have to diffuse to reach the surface. In 1D PCWs, this distance is determined primarily

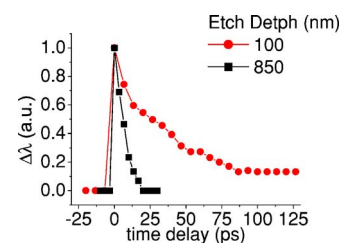


FIG. 4. (Color online) $\Delta\lambda$ vs probe time delay for the deep- and shallow-etched PCWs. Both samples had the same period of 330 nm and air-fill factor of 30%. The graphs have been normalized so that $\Delta\lambda$ is equal to unity at zero time delay.

by the stripe width, as demonstrated by the data shown in Figs. 3(a) and 3(b).

The inset to Fig. 3(b) shows the results of a simple in-plane model, which calculates the probability of a carrier reaching the surface based on the mean distance traveled by the carriers excited in AlGaAs. The model accurately reproduces the linear dependence on the stripe width. The carrier diffusion velocity¹⁶ and the carrier lifetime¹⁷ are taken to be 20 000 m/s and 100 ps, respectively. The former parameter controls how likely carriers are to reach any surface, whereas the latter is the recombination time of carriers that have not reached the surface. These parameters are material dependent. The simple nature of the model only allows for a qualitative agreement with the experimental data. A fully fledged three-dimensional analysis would be required to model the decay time quantitatively.

Figure 4 shows the dependence of the wavelength shift on the etch depth for a constant period of 330 nm and air-fill factor of 30%. The decay times in the deep- and shallow-etched structures were found to be 8 and 33.5 ps, respectively. This strong dependence on the etch depth can again be attributed to the surface recombination rate. The surface area of the deeply etched PCW was approximately 4.5 times larger than in the shallow-etched structure, and the ratio of the two decay times (4.2) is almost in direct proportion to this factor. The good correlation between the reduction in surface area and the increase in the decay time shows the effect of surface recombination in PCWs.

In conclusion, we have demonstrated that the free carrier response of 1D PCWs depends on the period, air-fill factor, and etch depth. The decay time was found to range between 8 and 26 ps when the stripe width was increased from 231 to 704 nm. Conversely, when the etch depth was re-

duced from 850 to 100 nm, the decay time increased from 8 to 33.5 ps. This work demonstrates that 1D PCWs are very good candidates for fast all-optical switches with highly customizable recovery times.

The authors would like to acknowledge support from the EPSRC via Grant No. GR/S76076.

¹E. Yablonovitch, Phys. Rev. Lett. **58**, 2059 (1987).

²S. John, Phys. Rev. Lett. **58**, 2486 (1987).

³For a recent review, see A. R. Cowan and J. F. Young, Semicond. Sci. Technol. **20**, R41 (2005).

⁴M. Scalora, J. P. Dowling, C. M. Bowden, and M. J. Bloemer, Phys. Rev. Lett. **73**, 1368 (1994).

⁵P. M. Johnson, A. F. Koenderink, and W. L. Vos, Phys. Rev. B **66**, 081102 (2002).

⁶S. Lan and H. Ishikawa, J. Appl. Phys. **91**, 2573 (2002).

⁷M. G. Banaee, A. R. Cowan, and J. F. Young, J. Opt. Soc. Am. B **19**, 2224 (2002).

⁸A. Hache and M. Bourgeois, Appl. Phys. Lett. **77**, 4089 (2000).

⁹S. R. Hastings, M. J. A. de Dood, H. Kim, W. Marshall, H. S. Eisenberg, and D. Bouwmeester, Appl. Phys. Lett. **86**, 031109 (2005).

¹⁰S. W. Leonard, H. M. Van Driel, J. Schilling, and R. B. Wehrspohn, Phys. Rev. B **66**, 161102 (2002).

¹¹M. Shimizu and T. Ishihara, Appl. Phys. Lett. **80**, 2836 (2002).

¹²H. W. Tan, H. M. van Driel, S. L. Schweizer, R. B. Wehrspohn, and U. Gosele, Phys. Rev. B **70**, 205110 (2004).

¹³A. D. Bristow, J. P. R. Wells, W. H. Fan, A. M. Fox, M. S. Skolnick, D. M. Whittaker, A. Tahraoui, T. F. Krauss, and J. S. Roberts, Appl. Phys. Lett. **83**, 851 (2003).

¹⁴A. D. Bristow, D. O. Kundys, A. Z. Garcia-Deniz, J. P. R. Wells, A. M. Fox, M. S. Skolnick, D. M. Whittaker, A. Tahraoui, T. F. Krauss, and J. S. Roberts, J. Appl. Phys. **96**, 4729 (2004).

¹⁵J. P. Mondia, H. W. Tan, S. Linden, H. M. van Driel, and J. F. Young, J. Opt. Soc. Am. B **22**, 2480 (2005).

¹⁶D. E. Aspnes, Surf. Sci. **132**, 406 (1983).

¹⁷M. J. LaGasse, K. K. Anderson, C. A. Wang, H. A. Haus, and J. G. Fujimoto, Appl. Phys. Lett. **56**, 417 (1990).